Heat Transfer Engineering

ISSN: 0145-7632 (Print) 1521-0537 (Online) Journal homepage: https://www.tandfonline.com/loi/uhte20

Heat Transfer Enhancement in a Microchannel Heat Sink: Nanofluids and/or Micro Pin Fins

Turgay Coşkun & Erdal Çetkin

To cite this article: Turgay Coşkun & Erdal Çetkin (2020) Heat Transfer Enhancement in a Microchannel Heat Sink: Nanofluids and/or Micro Pin Fins, Heat Transfer Engineering, 41:21, 1818-1828, DOI: 10.1080/01457632.2019.1670467

To link to this article: https://doi.org/10.1080/01457632.2019.1670467

HEAT TRANSFER ENGINEERING
2020, VOL. 41, NO. 21, 1818–1828
https://doi.org/10.1080/01457632.2019.1670467

Taylor & Francis
Taylor & Francis Group

Heat Transfer Enhancement in a Microchannel Heat Sink: Nanofluids and/or Micro Pin Fins

Turgay Coşkun and Erdal Çetkin

Department of Mechanical Engineering, Izmir Institute of Technology, Izmir, Turkey

ABSTRACT

Here, we show that overall thermal conductance in a rectangular microchannel heat sink can be maximized with the combination of nanofluids and micro pin fins. We uncover the effect of micro pin fins and nanofluids both separately and simultaneously in order to uncover their effect on the thermal conductance (i.e., thermal resistance). Both nanofluids and micro pin fins decrease the overall thermal resistance due to increase in the average thermal conductivity of the flow system. In addition, they increase the heat transfer surface area of the solid interacting with the fluid. However, the pumping power (pressure drop) increases in both methods due to the increase in the resistances to the fluid flow. The results document what should be the nanoparticle volume fraction mixed into the base fluid and the micro pin fin volume in order to minimize thermal resistance. If the thermal conductivity of the nanoparticles and micro pin fins are the same, the thermal conductance becomes the maximum with 4% and 0.14% volume fractions for the nanofluid and micro pin fins, respectively. This result shows that inserting micro pin fins and using nanofluids with a given volume fraction ratio maximize the overall thermal conductance.

Introduction

Advanced applications with miniature designs require great volumetric heating capabilities. Therefore, the literature focuses on maximization of thermal conductance (i.e., minimization of thermal resistances) when the reserved space for cooling system is limited. The literature also focuses on cooling with nanofluids and phase changing materials due to their capability of increasing thermal conductance [1–4]. In addition, the literature documents heat transfer enhancement with micro pin fins [5–12]. Nanofluid suspensions (base fluid + nanoparticles) have greater thermal conductivity relative to their base fluid because of the high thermal conductivity of suspended particles. The rate of enhancement in the thermal conductivity of base fluids is still a hotly debated topic. However, it is well known that the downside of nanofluids is that they increase pressure drop [13–24]. Likewise, the pressure drop along the microchannels with inserted micro pin fins [8–12].

Tuckerman and Pease [5] were first to investigate the performance of silicon based micro pin fins. They documented the pressure drop along microchannels for three distinct square fin designs. However, they did not document the thermal performance of fins. Peles et al. [6] experimentally uncovered the effect of micro pin fins on heat transfer rate and pressure drop. They documented the parameters which are affecting the overall thermal resistance. They showed that the thermal resistance can be decreased greatly (1.5–2.5 times) with inserted pin fin heat sinks. Koşar et al. [7] investigated the effect of staggered and inline micro pin fin bundles on pressure drop. They compared the micro scale pressure drop results with the macro scale data which evaluated based on conventional pressure drop correlations. In addition, they proposed a modified correlation for flow over micro pin fin bundles. Adewumi et al. [8] documented what the size of embedded micro pin fins should be to minimize thermal resistance. Prasher et al. [9] experimentally uncovered the thermal and hydraulic performances of silicon-based, low aspect ratio micro pin fin bundles under cross flow. They showed how the average Nusselt number (Nu) and friction factor vary relative to the fin diameter. Qu and Siu-Ho [10, 11] surveyed how the heat transfer rate and pressured drop vary with micro pin fin arrays. First [10], they

CONTACT Associate Professor Erdal Çetkin erdalcetkin@iyte.edu.tr Department of Mechanical Engineering, Izmir Institute of Technology, Izmir, Turkey.
Color versions of one or more of the figures in the article can be found online at www.tandfonline.com/uhte.

Nomenclature

Be	Bejan number	x, y, z	Cartesian coordinates (m)
C_p	specific heat (J/kg·°C)	***Greek symbols***	
D	diameter (m)	A	Thermal diffusivity (m^2/s)
H	height (m)	M	Dynamic viscosity (kg/m. s)
L	length (m)	ρ	Density (kg/m^3)
K	thermal conductivity (W/m·°C)	$\emptyset$	volume fraction
N	normal vector	***Subscripts***	
Nu	Nusselt number	atm	atmospheric conditions
$P_{"}$	pressure (Pa)	C	channel
q	heat transfer per unit area (W/m^2)	eff	effective
Q	volume flow rate (m^3/s)	F	fluid
T	temperature (°C)	I	index
U	velocity in x-direction (m/s)	In	inlet
V	velocity in y-direction (m/s)	N	any number
$\vec{v}$	velocity vector	out	outlet
V	volume (m^3)	S	solid
W	velocity in z-direction (m/s)	T	total
W	width (m)		

proposed two Nusselt number correlations and compared them with the existing correlations. Then [11], they developed a power-law type correlation to predict average Nu number for adiabatic and diabatic conditions.

Nanofluids were introduced by Choi and Eastman [13]. They observed the that the average thermal conductivity of a fluid with suspended copper particle increases. Choi et al. [14] showed that the thermal conductivity of a base fluid increases approximately two times by addition of less than 1% carbon nanotubes. Prasher et al. [15] documented how the viscosity of alumina-based nanofluid is affected by shear rate, temperature, nanoparticle diameter and volume fraction. They concluded that increase in the viscosity is greater than (50%) the increase in the thermal conductance. Xuan et al. [16] experimentally uncovered the enhancement in the thermal conductivity of a copper and water suspension. They also investigated the effect of particle aggregation on thermal conductivity of nanofluids. Nguyen et al. [17] documented the dynamic viscosity of Al_2O_3/water nanofluid for the temperature range of 20 °C to nearly 75 °C. Anoop et al. [18] investigated the heat transfer enhancement in laminar developing region for various size and concentration of nanoparticles. Das et al. [19] comprehensively reviewed the nanofluid literature. They stated that there is not a certain equation nor approach which gives the change in the thermal conductivity with nanoparticle addition to a base fluid. Buongiorno et al. [20] emphasized that the literature does not agree on the thermal properties of nanofluids. In order to resolve inconsistencies, an international nanofluid property benchmark exercise (INPBE) was launched at the first scientific conference which focuses on nanofluids. By this way, it was agreed that thermal conductivity and other properties of nanofluids would be tested by over 30 organizations worldwide; and the results would be reported by publications. Chandrasekar et al. [21] measured the thermal conductivity and viscosity of Al_2O_3/water nanofluid in the volume fraction range from 0.33% to 5%. They concluded that both properties increase linearly as the volume concentration increases. In addition, increase in the viscosity becomes nonlinear after 2% volume concentration because of the hydrodynamic interactions between nanoparticles and base fluid. Later, Chandrasekar et al. [22] uncovered the change of pressure drop under constant heat flux condition in the plane tube with a 0.1% volume fraction nanofluid (Al_2O_3-water suspension). They observed 34% increase in the Nusselt number; and they did not observe a significant increase in the pressure drop with nanofluids compared to distilled water. Lin et al. [23] numerically surveyed pressure drop and heat transfer rate of nanofluids (water/Al_2O_3 suspension) in turbulent pipe flow. They stated that distribution of nanoparticles in the flow field becomes nonuniform due to the particle convection, diffusion, coagulation and breakage. They observed Nusselt number decreased by 8% and 3% because of the nonuniformity with Reynolds numbers of 5000 and 25000, respectively. Yuan et al. [24] numerically uncovered how the volume fraction of cylindrical nanoparticles affect the viscosity of the nanofluid. They showed that resistance to the fluid flow increases with volume fraction; however, the effect of volume fraction diminishes when Reynolds number is greater than 200. Ghanbarpour et al. [25] experimentally uncovered the thermal properties and rheological behavior of water

based Al_2O_3 nanofluids. They showed that thermal conductivity and viscosity of nanofluids increase as temperature and/or particle concentration increase. However, they documented that the increase in the viscosity is more pronounced than the increase in the thermal conductivity. Karimzadehkhouei et al. [26] numerically and experimentally investigated the effect of inlet temperature of Al_2O_3 suspension on heat transfer rate along microchannels. They concluded that the effect of inlet temperature on the heat transfer rate is dominant near the inlet of channels (<L/5).

The current literature shows that both fins and nanofluids increase the resistance to fluid flow and decrease the resistance to heat flow. However, it focuses on the effect of micro pin fins and nanofluids separately. Here we uncover what should be the ratio of solid volume reserved for fins and nanoparticles when they both exist in order to enhance the overall thermal conductance (minimization of thermal resistance) with minimum pressure drop. Recent studies emphasize that the nanofluid thermofluidic properties should be measured via experiments, such as thermal conductivity, viscosity etc. Therefore, here we benefit from the experimental results of Chandrasekar et al. [21].

Model

The physical model consists of a microchannel with length scales of $L \times W_c \times H_c$, which is inserted in a silicone substrate with length scales of $L \times W \times H$ as shown in Figures 1a–b. Figure 1b shows how the micro pin fins are inserted into the microchannel. The material of the micro pin fins is highly conductive silicon substrate. The micro pin fins are circular cylinders with diameter of D_{fin} and height of H_{fin}. The volume of the microchannel is fixed, and so is the volume of the solid domain surrounding it. Length scales of the computational domain are given in Table 1. Two physical models were used in the present study. First one is the microchannel heat sink without micro pin fins and the second one is with them, i.e. integrated design.

The volume of the computational domain is fixed, which is

$$L \times W \times H = 9 \text{ mm}^2 \quad (1)$$

The number of fins inserted into the microchannel can vary but total fin volume is fixed,

$$V_{fin,t} = V_{fin,1} + V_{fin,2} + \ldots + V_{fin,n} = 6.03 \times 10^{-4} \text{ mm}^3 \quad (2)$$

The height (H_{fin}) and the diameter of the fins (D_{fin}) are 0.08 mm and 0.04 mm, respectively. The total fin volume is 0.14% of the total solid volume.

Governing equations

The coolant in the simulations are pure water or nanofluid (water-Al_2O_3 suspension). Water and nanofluid are incompressible with homogeneous and constant thermophysical properties. The effect of buoyancy forces is negligibly small in the current problem due to the micro length scales.

Table 1. Dimensions of the solid and fluid domains.

Solid domain			Fluid domain	
H (mm)	W (mm)	L (mm)	H_c (mm)	W_c (mm)
0.9	0.1	10	0.705	0.06

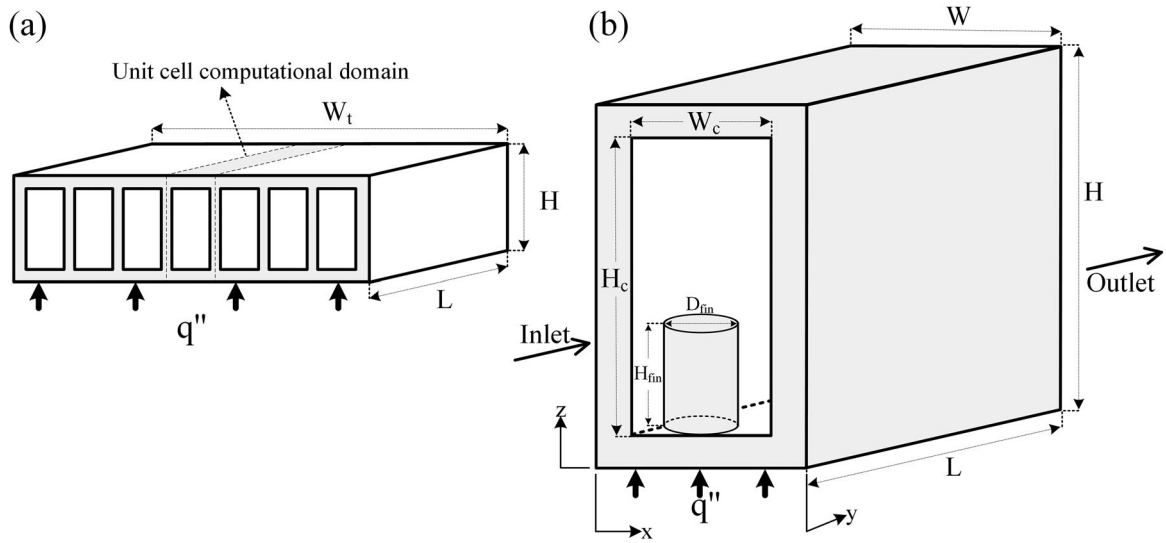

Figure 1. Physical model of microchannel heat sink: (a) stacked model and (b) computational domain.

Conservation of mass, momentum and energy equations were solved numerically to determine velocity and temperature distribution for the solution domain. For laminar and steady flow, the governing equations are;

$$\nabla.\vec{v} = 0 \tag{3}$$

$$\rho_f(\vec{v}.\nabla\vec{v}) = -\nabla P + \mu_f\nabla^2\vec{v} \tag{4}$$

$$\rho_f C_{p,f}(\vec{v}.\nabla T) = k_f\nabla^2 T \tag{5}$$

where ρ_f, $C_{p,f}$, k_f, μ_f are the density, specific heat, thermal conductivity and dynamic viscosity of the fluid. $\vec{v}$ is the velocity vector in the fluid domain.

For solid regions, the energy equation reduces to:

$$k_s\nabla^2 T = 0 \tag{6}$$

where k_s is the thermal conductivity in the solid domains (i.e., the thermal conductivity of solid channel and fins).

Boundary conditions

The coolant is driven by the pressure difference in between the inlet and outlet surfaces of the microchannel as shown in Figure 1b. The pressure difference is defined as

$$P_{in} = \frac{Be \times \alpha \times \mu}{V^{2/3}} + P_{out} \tag{7}$$

α, V, and P_{out} are thermal diffusivity of the fluid, volume of the computational domain and pressure at the microchannel outlet, respectively. In addition, Be is Bejan number [27, 28] which represents the dimensionless pressure difference along a channel. It was derived during the channel size optimization in forced convection. Furthermore, Bejan and Lorente [29] emphasized that the role played by the Rayleigh number for the natural convection cooling is played by Bejan number in forced convection, cf. pp. 92 of Ref. [29]. Be number is defined in Petrescu [28] as

$$Be = \frac{\Delta P \times L^2}{\mu \times \alpha} \tag{8}$$

The boundaries of the microchannel surrounded by the solid surface is defined as no slip wall boundaries with stationary wall

$$u = v = w = 0 \tag{9}$$

The outlet boundary is defined as pressure outlet ($y = L$),

$$P_{out} = P_{atm} \tag{10}$$

The temperature of the coolant at the inlet boundary ($y = 0$) is fixed.

$$T_{in} = 20^{\circ}C \tag{11}$$

The left and right boundaries of the domain ($x = 0$ and $x = W$) are symmetry boundaries,

$$\partial T/\partial x = 0 \tag{12}$$

At the bottom wall ($z = 0$), uniform heat flux is applied,

$$q'' = k_s\frac{\partial T}{\partial y} = 10^6 \ W/m^2 \tag{13}$$

The remaining outside walls of the solid domain surrounding the microchannel are adiabatic. The continuity of energy at the interfaces of solid and fluid surfaces satisfy

$$k_s\frac{\partial T}{\partial n_{wall}} = k_f\frac{\partial T}{\partial n_{wall}} \tag{14}$$

where n is the outward normal vector.

Nanofluid

Density, specific heat, viscosity and thermal conductivity of the working fluid are function of volume fraction of the suspended nanoparticle. The effective density and specific heat values for nanofluids calculated from the following equations [30]:

$$\rho_{eff} = \emptyset\rho_s + (1-\emptyset)\rho_f \tag{15}$$

$$C_{p,eff} = \emptyset C_{p,s} + (1-\emptyset)C_{p,f} \tag{16}$$

where Ø is the volume fraction of the nanoparticle.

One of the important thermophysical parameters of nanofluids is viscosity which affects the pressure drop. Viscosity of a nanofluid depends on nanoparticle volume fraction, its diameter and temperature [15]. Similarly, nanoparticle size, shape, temperature, particle interaction between the solid and fluid are the main parameters affecting the thermal conductivity of the nanofluids [19, 31]. In the literature, there are many equations to calculate effective viscosity and thermal conductivity of nanofluids. However, the literature shows that the nanofluid material properties vary dramatically between models in published documents. Experimentally measured nanofluid thermophysical properties were used during the study (cf. experimental results of Chandrasekar et al. [21]) in order to understand the effect of nanofluids in the heat transfer enhancement clearly without the effect of bias in the material model. Thermophysical properties of the base fluid (water) and nanoparticles (Al_2O_3) are given in Table 2 [21, 30, 32, 33].

Table 2. Thermophysical properties of water and Al_2O_3 at 20 °C [21, 30, 32, 33].

	K (W/m· °C)	ρ (kg/m^3)	C_p (J/kg· °C)	μ (kg/m·s)
Water	0.6	997	4170	0.00100
Al_2O_3	35	3880	729	–
Nanofluid (0.1%)	0.621	1025.8	4135.6	0.00110
Nanofluid (0.2%)	0.630	1057.7	4113.5	0.00121
Nanofluid (0.3%)	0.658	1083.5	4066.8	0.00140
Nanofluid (0.4%)	0.695	1112.3	4032.4	0.00170

Table 3. Relative error corresponding to the number of mesh elements for the base model.

Number of mesh elements	ΔT (°C)	$\left[\frac{(\Delta T)_i-(\Delta T)_{i-1}}{(\Delta T)_i}\right]$
37782	14.9329	–
86867	15.1366	0.0135
264372	15.3619	0.0147
460318	15.4670	0.0068

Numerical procedure

The conservation of mass, momentum and energy equations were solved numerically by using a commercial finite element software, COMSOL Multiphysics 5.0 [34]. The computational domain was meshed using free tetrahedral and pyramid elements. The convergence criteria were specified as 10^{-5} for continuity, momentum and energy equations during the simulations. The simulation results are considered as mesh independent when the criterion of Eq. (17) is satisfied.

$$\left[\frac{(\Delta T)_i-(\Delta T)_{i-1}}{(\Delta T)_i}\right] \leq 0.01 \qquad (17)$$

Here, ΔT is defined as the difference between maximum and minimum temperatures of the fluid, and "i" represents the mesh index. The effect of mesh size on the simulation results of base model and integrated model are represented in Tables 3 and 4, respectively.

Validation of the model

Validation of the model is carried out with respect to the literature. Figure 2 shows the comparison between the results of Adewumi et al. [8], Bello-Ochende et al. [35], and the present study. The accuracy of Adewumi et al. [8] and Bello-Ochende et al. [35] were given as 10% and 15% with respect to the analytical results of Khan et al. [36] and experimental results of Tuckerman and Pease [5], respectively. The figure shows that the values obtained in the present study are in good agreement with the studies of Adewumi et al. [8] and Bello-Ochende et al. [35] with an average deviation of about 7.3% and 2.6%, respectively.

Table 4. Relative error corresponding to the number of mesh elements for the integrated design.

Number of mesh elements	ΔT (°C)	$\left[\frac{(\Delta T)_i-(\Delta T)_{i-1}}{(\Delta T)_i}\right]$
51893	14.7852	–
230569	14.9877	0.0135
438920	15.1653	0.0117
585770	15.1812	0.0010

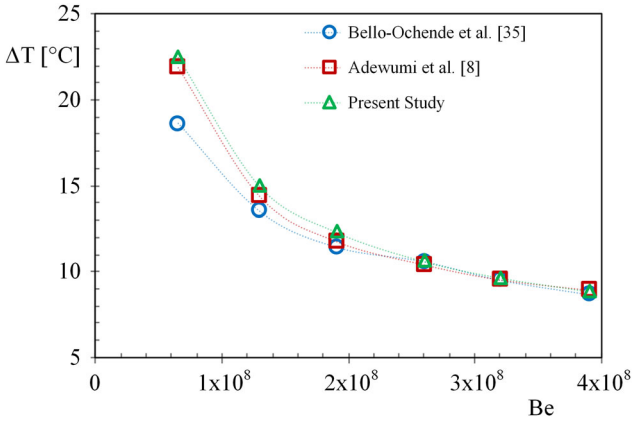

Figure 2. Comparison between results of presented model and literature for wall temperature differences.

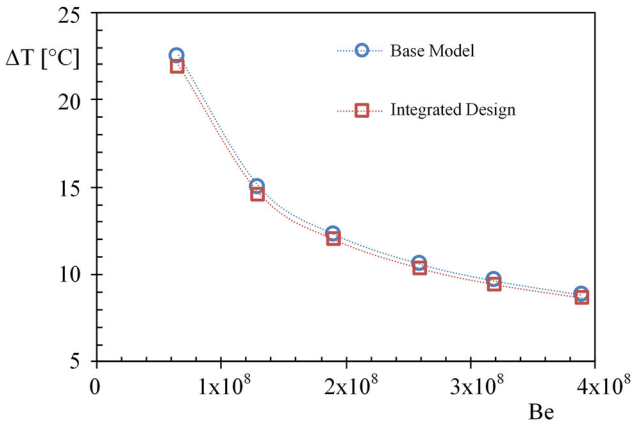

Figure 3. Influence of dimensionless pressure drop on the peak wall temperature differences for base model and integrated design.

Heat transfer enhancement by fins

Figure 3 shows the effect of inserted micro pin fins on the peak temperature relative to the Be number. The figure reveals that 2.5% improvement was achieved by integrated design relative to the base model. The effect of integrated design on the thermal conductance diminishes as Be number increases. This result implies that at low Be numbers, heat transfer is limited due to low fluid velocity. Fins increase the heat transfer surface area; therefore, the heat transferred in integrated design is greater even the resistance to the fluid flow is greater. In addition, if the pressure drop related with the extended surface

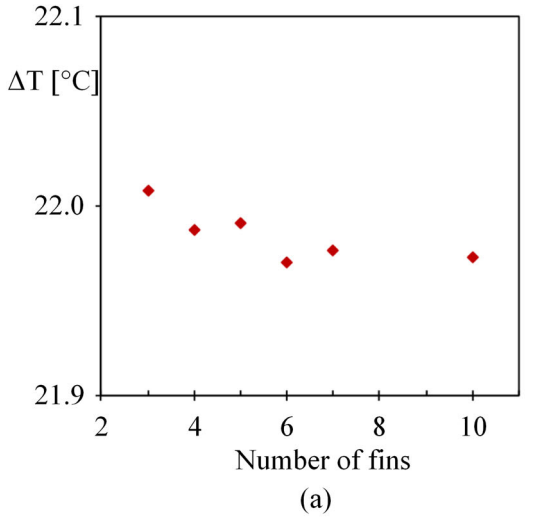

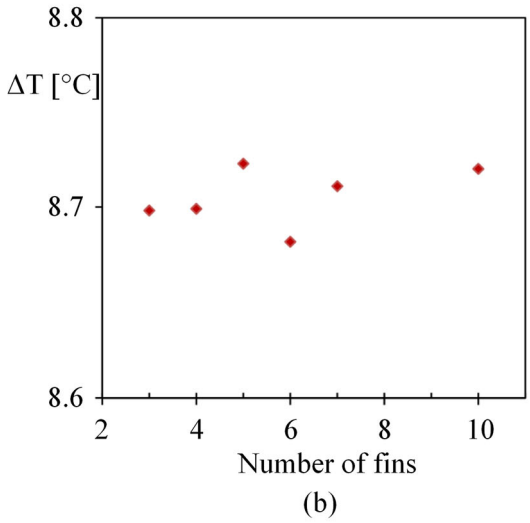

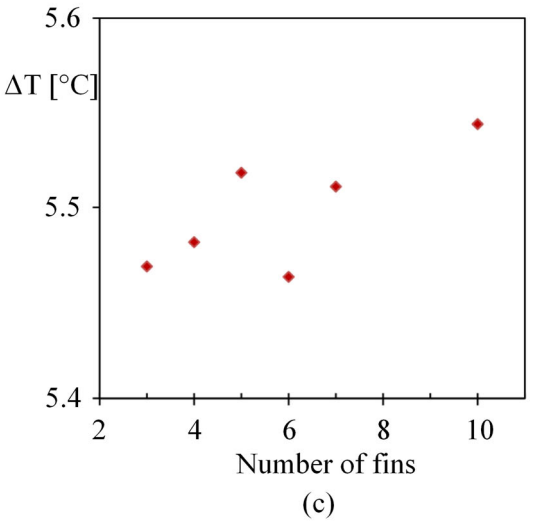

Figure 4. Variation of the peak wall temperature differences with fin numbers for: (a) Be = 6.5×10^7, (b) Be = 3.9×10^8, (c) Be = $1.3 \times .10^9$.

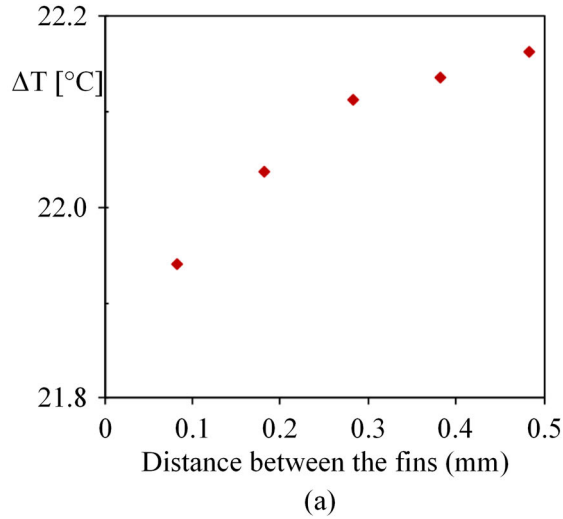

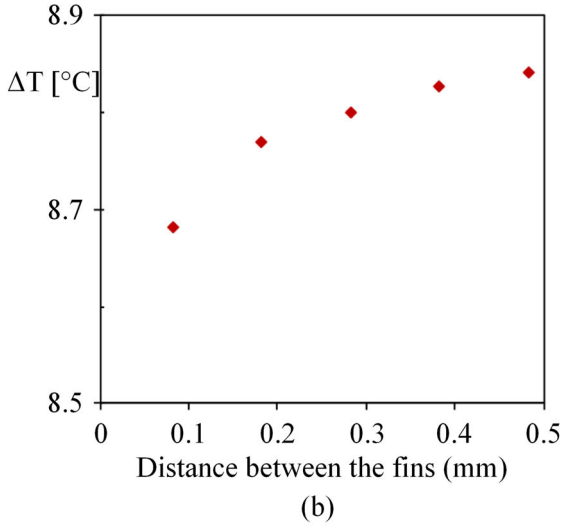

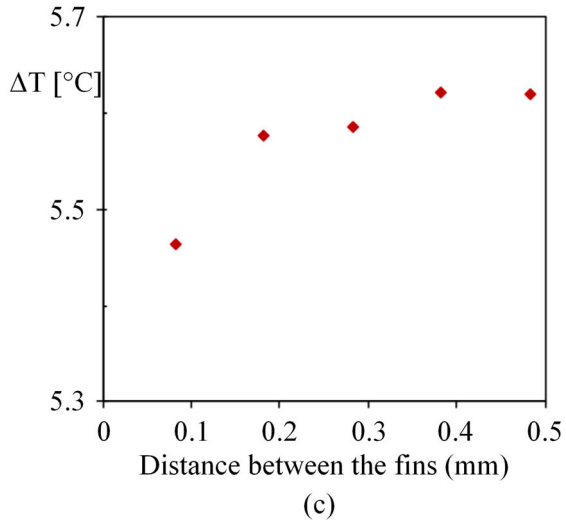

Figure 5. Variation of the peak wall temperature differences with the distance between the fins for: (a) Be = 6.5×10^7, (b) Be = 3.9×10^8, (c) Be = $1.3 \times .10^9$.

dramatically decreases the fluid velocity, then the base model may provide smaller thermal resistance than the integrated design.

First fin in the integrated design is centered nearly to the inlet of the microchannel and the rest of the fins were aligned with a fixed distance from each other

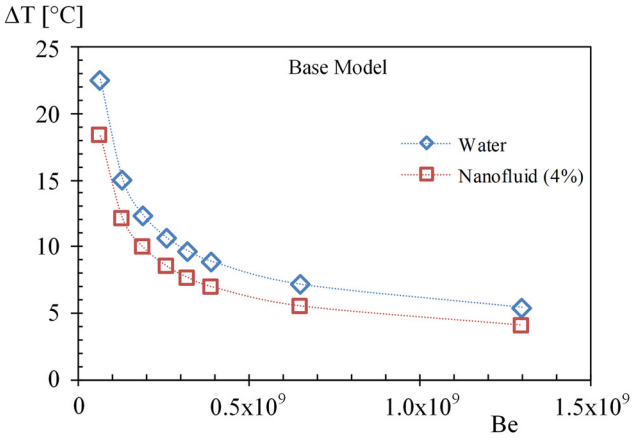

Figure 6. Variation of the peak wall temperature differences with Be number for Base Model.

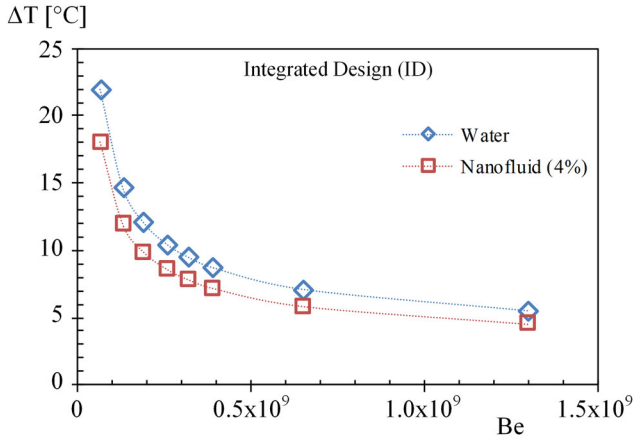

Figure 7. Variation of the peak wall temperature differences with Be number for Integrated Design.

along the microchannel. The optimum fin numbers and the distance between the fins were determined with respect to the minimized peak wall temperature difference. Figure 4a shows that the peak temperature decreases as the number of fins increases until the 6th fin when Be $= 6.5 \times 10^7$. Then, the peak temperature stands almost steady. Figure 4b,c also show that the peak temperature is the smallest for the 6th micro pin fin; and increasing the fin number increases the peak temperature (thermal resistance) afterwards. Overall, according to Figure 4, the integrated design with 6 micro pin fins minimizes the peak wall temperature differences (maximum thermal conductance) for low, intermediate and high Be numbers.

Figure 5 shows the effect of distance between the fins on peak wall temperature difference for 6 fins. According to Figure 5, the peak wall temperature difference is minimum when the distance between the fins is 0.0825 mm for all Be numbers. In Figure 5, it can be seen that the peak wall temperature difference increases as the distance between the fins increases. This result implies that as the distance between the fins increases, the next level of fins stays in the wake of the previous fins due to the increase in the thermal boundary layer. Furthermore, as the fluid flows along the channel its temperature increases, which decreases the heat transfer rate from the fins to fluid. Therefore, the effect of fins on heat transfer rate diminishes as the spacing in between them increases.

Heat transfer enhancement by nanofluid

Next consider the coolant is a nanofluid (suspension of water and Al_2O_3) with various volume fractions. Figure 6 shows that the peak temperature difference decreases with 4% Al_2O_3 nanoparticle addition to the water. The effect of nanofluid on the peak temperature difference is more pronounced at low Be numbers. However, 18% and 25% improvements were observed in minimizing the peak wall temperature difference by using nanofluid for Be numbers 6.5×10^7 and 1.3×10^9, respectively. Note that Be number (dimensionless pressure difference) is fixed throughout the study; therefore, change in the pressure drop is related to the variation in the material properties as can be seen in Eq. (7).

Figure 7 shows the effect of nanofluid on the peak wall temperature difference for the integrated design. Similar to the base model (Figure 6), nanofluid increases the overall thermal conductance for all Be numbers; however, increase in the thermal conductance for the integrated design diminishes as the Be number increases. Maximum improvement in the peak wall temperature difference was measured as 18% for the lowest Be number, 6.5×10^7.

Comparison of Figures 6 and 7 reveals that the enhancement in the thermal conductance is greater in base model than the integrated one for the greatest Be number. However, the integrated design yields better enhancement in the thermal conductance as the Be number decreases. This shows that only fins yield better thermal performance at low Be numbers, and only nanofluid at high Be numbers. Therefore, there is an optimal volume fraction ratio at the intermediate Be numbers.

The effect of nanofluid volume fraction on the peak wall temperature differences is represented in Figure 8a–c for the lowest, intermediate and highest Be numbers. Volume fraction of nanofluid varies from 1% to 4%. In general, Figure 8a–c show that thermal conductance increases as the nanoparticle volume fraction in the fluid increases, with the exception of Figure 8a. Figure 8a is for the lowest Be number case; therefore, increase in the flow resistance limits the enhancement in thermal conductance via

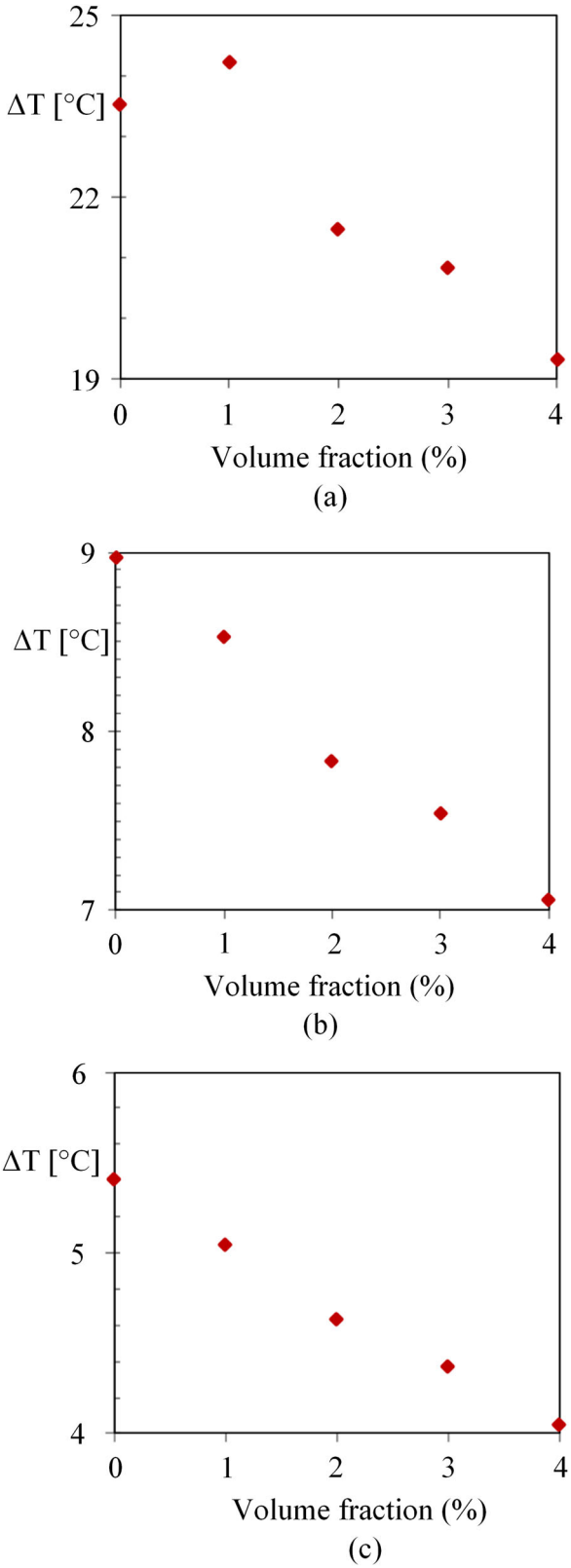

Figure 8. Variation of the peak wall temperature differences with nanofluid volume fraction for various Be numbers; (a)6.5×10^7 (b) 3.9×10^8 (c) $1.3 \times .10^9$.

nanofluids. The minimum wall temperature differences are observed in 4% volume fraction. The volume fraction was limited as 4% in order to eliminate

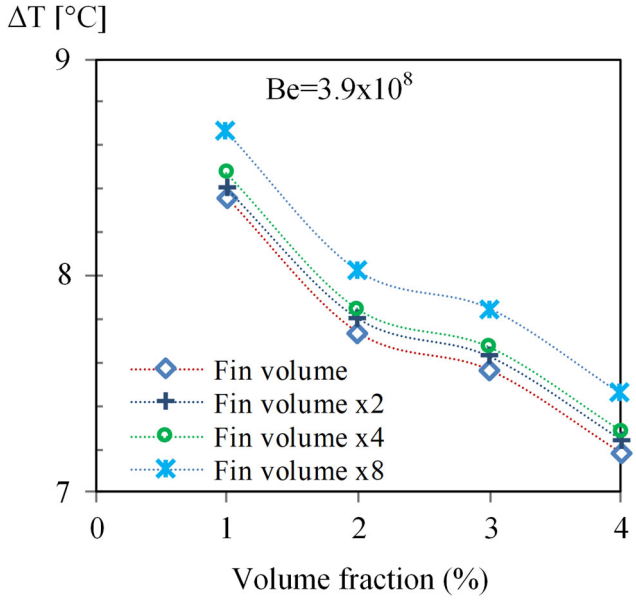

Figure 9. Variation of the peak wall temperature differences with volume fraction of nanofluid and total fin volume.

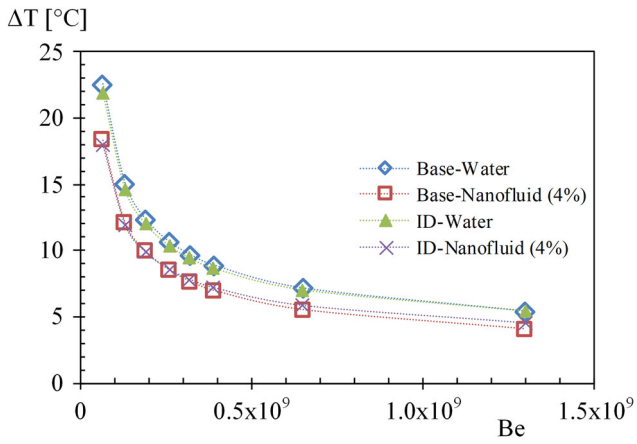

Figure 10. Peak wall temperature differences relative to Be number with and without nanofluids for base model and integrated design.

agglomeration in the nanofluid. Figure 8 shows that utilizing nanofluid is an ineffective solution to reduce peak wall temperature differences for the lowest Be number at 1% volume fraction. Maximum improvement in the peak wall temperature difference is 25% in the highest Be number for 4% volume fraction. However, the pressure drop increases dramatically as the volume fraction increases from 1 to 4%, i.e. 10.3% to 45.4% increase compared to the base fluid, respectively.

The effect of total fin volume and volume fraction of nanofluid on the temperature difference is shown in Figure 9. The peak wall temperature difference decreases by increasing the volume fraction of nanofluid while fin volume is fixed. However, increasing the total volume of the fins decreases the thermal

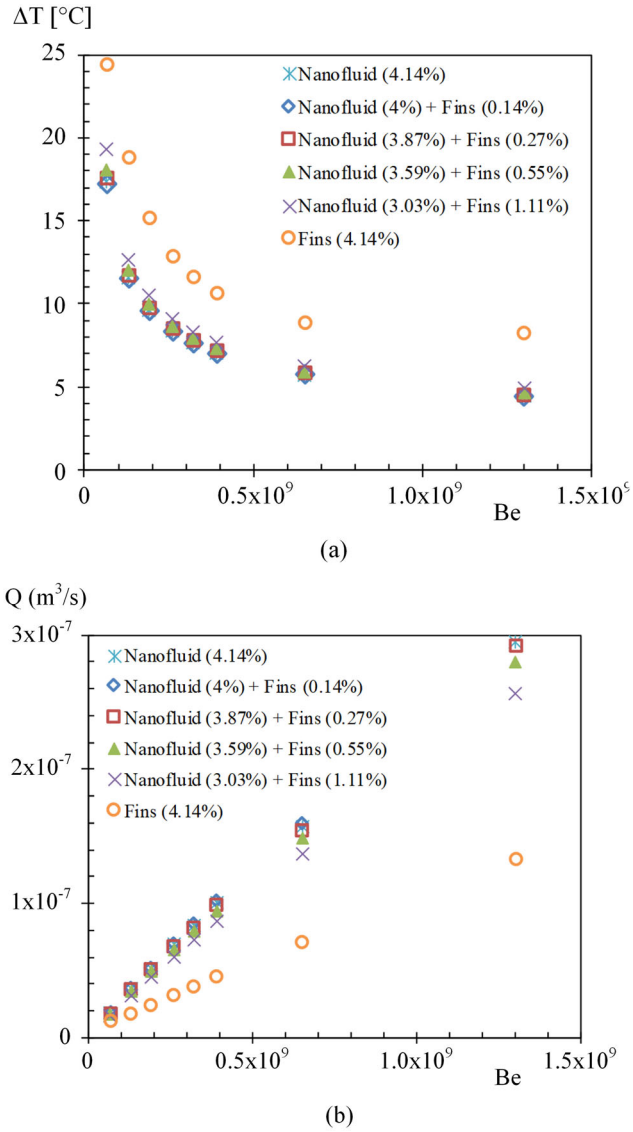

Figure 11. The change in (a) the peak wall temperature difference and (b) the volumetric flow rate of the coolant with respect to volume fraction of nanofluid and total fin volume.

conductance. For instance, 3.8% increment in the wall temperature is observed when the fin volume increases eight times. This situation can be explained as an increase in the total fin volume increases the resistance to the fluid flow, which decreases convective heat transfer coefficient.

Figure 10 summarizes the results of the study. According to Figure 10, integrated design with nanofluid minimizes the peak wall temperature difference for the lowest Be number. In addition, base model with water yields the greatest peak wall temperature difference for the lowest Be number. Furthermore, base model with nanofluid minimizes the peak temperature difference for the highest Be number. Therefore, it can be concluded that thermal conductance is maximum with fins and nanofluid, and nanofluid for low and high Be numbers. Therefore, nanofluid should be used with or without fins relative to the given Be number in order to maximize the thermal conductance. For instance, if an evolutionary analogy is used, it means that particles forming the fins dissolves in time to enhance heat transfer rate.

Next, consider that the thermal conductivities of the nanoparticle and fins are the same (35 W/m·K) in order to understand the evolutionary concept. Figure 11 shows how the temperature difference and volumetric flow rate vary relative to the Be number for fins, nanofluids and fins + nanofluids with fixed volume fraction. So far, the fin volume was 0.14% and the maximum nanofluid volume fraction was 4%. Here, the summation of the volumes of fins and nanoparticles correspond to 4.14% volume fraction. Therefore, the optimal ratio of volume fraction between the fins and nanofluid for thermal conductance enhancement becomes evident.

According to Figure 11, nanofluid yields the maximum thermal conductance (almost 50% improvement in the thermal conductance relative to the micro pin fins) by minimizing the peak wall temperature difference. Figure 11a shows that the thermal conductance with only fins (4.14% volume fraction) is smaller in comparison to the only nanofluid (4.14% volume fraction) whereas their resistance to the fluid flow is greater (decreased volumetric flow rate "Q" for the same Be number). Figure 11a–b show that suspending the majority of the solid volume into the fluid enhances thermal conductance more than embedding micro pin fins; and, it also minimizes resistance to the fluid flow. However, Figure 11a,b also show that greatest thermal conductance and the smallest resistance to the fluid flow is achieved when a small percentage (0.14% volume fraction) of the solid volume is reserved for fins.

Conclusions

Here, we document what should be the volume fractions of micro pin fins and nanoparticles to conform maximum thermal conductance for a microchannel heat sink. The effect of fins and nanoparticles suspended to the base fluid (water) on the thermal conductance documented both solely and simultaneously. The results show that microchannel with micro pin fins provides greater thermal conductance than microchannel without micro pin fins. The distance between the fins and their number were optimized to maximize thermal conductance. Heat transfer enhancement with nanofluid is also documented for various Be

numbers. The results show that nanofluid with volume fraction of 4% significantly reduce the peak temperature. Nanofluid with any volume fraction improve the thermal conductance for all the surveyed Be numbers. However, nanofluid also increases the resistance to the fluid flow which requires additional pumping power. Nanofluid with micro pin fins increases the thermal conductance by 18% for the lowest Be number relative to the base fluid without fins. Increase in the total fin volume increases the resistances to the fluid flow, and therefore it increases the temperature difference of the microchannel up to 3.8%.

Nanofluid decreases the peak temperature more than inserting micro pin fins when the thermal conductivity of nanoparticles and micro pin fins are the same. Almost 50% improvement is achieved with nanofluid instead of micro pin fins. Overall, the results uncover that there is an optimum volume fraction reserved for fins and nanoparticles suspended in the base fluid for a prescribed set of conditions. Depending on the material properties of substances, the volume fractions which provide the minimum peak temperature (maximum thermal conductance) is affected.

Notes on contributors

Turgay Coskun is currently Research Assistant and Ph.D. student at Izmir Institute of Technology, Izmir, Turkey. He received his B.S. degree in Mechanical Engineering in 2013 and his M.Sc. degree in Energy Engineering in 2016 from the same university. His research interests include heat transfer in microchannels and nanofluids.

Erdal Cetkin is a Professor of Faculty of Engineering at Izmir Institute of Technology, Izmir, Turkey. He received his Ph.D. in Thermofluidics in 2013 from Duke University, Durham, N.C., USA. He is currently working on heat transfer enhancement methods, heat transfer with phase change materials, mass transfer in micromixers and manifold design optimization.

References

1. M. Shafahi, V. Bianco, K. Vafai, and O. Manca, "Thermal performance of flat-shaped heat pipes using nanofluids," *Int. J. Heat Mass Transfer*, vol. 53, no. 7–8, pp. 1438–1445, 2010. DOI: 10.1016/j.ijheatmasstransfer.2009.12.007.
2. Y. Li, H. Q. Xie, W. Yu, and J. Li, "Liquid cooling of tractive lithium ion batteries pack with nanofluids coolant," *J. Nanosci. Nanotechnol.*, vol. 15, no. 4, pp. 3206–3211, 2015. DOI: 10.1166/jnn.2015.9672.
3. W. G. Alshaer, S. A. Nada, M. A. Rady, E. P. Del Barrio, and A. Sommier, "Thermal management of electronic devices using carbon foam and PCM/nanocomposite," *Int. J. Thermal Sci.*, vol. 89, pp. 79–86, 2015. DOI: 10.1016/j.ijthermalsci.2014.10.012.
4. T. Ma, H. X. Yang, Y. P. Zhang, L. Lu, and X. Wang, "Using phase change materials in photovoltaic systems for thermal regulation and electrical efficiency improvement: A review and outlook," *Renew. Sustain. Energy Rev.*, vol. 43, pp. 1273–1284, 2015. DOI: 10.1016/j.rser.2014.12.003.
5. D. B. Tuckerman, and R. F. W. Pease, "Ultrahigh thermal conductance microstructures for cooling integrated circuits," in Proc. 32nd Electronics Components Conf., San Diego, CA, 1981, pp. 145–149.
6. Y. Peles, A. Kosar, C. Mishra, C.-J. Kuo, and B. Schneider, "Forced convective heat transfer across a pin fin micro heat sink," *Int. J. Heat Mass Transfer*, vol. 48, no. 17, pp. 3615–3627, 2005.DOI: 10.1016/j.ijheatmasstransfer.2005.03.0.
7. A. Kosar, C. Mishra, and Y. Peles, "Laminar flow across a bank of low aspect ratio micro pin fins," *J. Fluids Eng.*, vol. 127, pp. 419–430, May 2005. DOI: 10.1115/1.1900139.
8. O. O. Adewumi, T. Bello-Ochende, and J. P. Meyer, "Constructual design of combined microchannel and micro pin fins for electronic cooling," *Int. J. Heat Mass Transfer*, vol. 66, pp. 315–323, 2013. DOI: 10.1016/j.ijheatmasstransfer.2013.07.039.
9. R. S. Prasher *et al.*, "Nusselt number and friction factor of staggered arrays of low aspect ratio micropin-fins under cross flow for water as fluid," *J. Heat Transfer, Trans. ASME*, vol. 129, no. 2, pp. 141–153, 2006. DOI: 10.1115/1.2402179.
10. W. Qu, and A. Siu-Ho, "Liquid single-phase flow in an array of micro-pin-fins-Part I: Heat transfer characteristics," *J. Heat Transfer, Trans. ASME*, vol. 130, no. 12, pp. 122–402, Sept. 2008. DOI: 10.1115/1.2970080.
11. W. Qu, and A. Siu-Ho, "Liquid single-phase flow in an array of micro-pin-fins-Part II: Pressure drop characteristics," *J. Heat Transfer, Trans. ASME*, vol. 130, no. 12, pp. 124501, Sept. 2008. DOI: 10.1115/1.2970082.
12. O. O. Adewumi, T. Bello-Ochende, and J. P. Meyer, "Comparison between the thermal performance of single and two-layer microchannels inserted with micro pin fins," presented at 15th Heat Transfer Conf., IHTC-15, Kyoto, Japan, Aug. 10–15, 2014.
13. S. U. S. Choi, and J. A. Eastman, "Enhancing thermal conductivity of fluids with nanoparticles," *ASME-Publ.-Fed*, vol. 231, pp. 99–106, 1995.
14. S. U. S. Choi, Z. G. Zhang, W. Yu, F. E. Lockwood, and E. A. Grulke, "Anomalous thermal conductivity enhancement in nanotube suspensions," *Appl. Phys. Lett.*, vol. 79, no. 14, pp. 2252–2254, 2001. DOI: 10.1063/1.1408272.
15. R. Prasher, D. Song, J. Wang, and P. Phelan, "Measurements of nanofluid viscosity and its

implications for thermal applications," *Appl. Phys. Lett.*, vol. 89, no. 13, pp. 133103–133108, 2006. DOI: 10.1063/1.2356113.
16. Y. Xuan, Q. Li, and W. Hu, "Aggregation structure and thermal conductivity of nanofluids," *AIChE J.*, vol. 49, no. 4, pp. 1038–1043, 2003. DOI: 10.1002/aic.690490420.
17. C. T. Nguyen *et al.*, "Viscosity data for Al_2O_3-water nanofluid-hysteresis: Is heat transfer enhancement using nanofluids reliable?," *Int. J. Therm. Sci.*, vol. 47, no. 2, pp. 103–111, 2008. DOI: 10.1016/j.ijthermalsci.2007.01.033.
18. K. B. Anoop, T. Sundararajan, and S. K. Das, "Effect of particle size on the convective heat transfer in nanofluid in the developing region," *Int. J. Heat Mass Transfer*, vol. 52, no. 9–10, pp. 2189–2195, 2009. DOI: 10.1016/j.ijheatmasstransfer.2007.11.063.
19. S. K. Das, S. U. S. Choi, and H. E. Patel, "Heat transfer in nanofluids—A review," *Heat Transfer Eng.*, vol. 27, no. 10, pp. 3–19, 2006. DOI: 10.1080/01457630600904593.
20. J. Buongiomo *et al.*, "A benchmark study on the thermal conductivity of nanofluids," *J. Appl. Phys.*, vol. 106, no. 094312-1, pp. 14, Nov. 2009. DOI: 10.1063/1.3245330.
21. M. Chandrasekar, S. Suresh, and A. Chandra Bose, "Experimental investigations and theoretical determination of thermal conductivity and viscosity of Al_2O_3/water nanofluid," *Exp. Therm. Fluid Sci.*, vol. 34, no. 2, pp. 210–216, 2010. DOI: 10.1016/j.expthermflusci.2009.10.022.
22. M. Chandrasekar, S. Suresh, and A. C. Bose, "Experimental studies on heat transfer and friction factor characteristics of Al_2O_3/water nanofluid in a circular pipe under transition flow with wire coil inserts," *Heat Transf. Eng.*, vol. 32, no. 6, pp. 485–496, 2011. DOI: 10.1080/01457632.2010.506358.
23. J. Lin, Y. Xia, and X. Ku, "Pressure drop and heat transfer of nanofluid in turbulent pipe flow considering particle coagulation and breakage," *J. Heat Transf.*, vol. 136, no. 11, pp. 111–701, 2014. DOI: 10.1115/1.4028325.
24. F. Yuan, J. Lin, and X. Ku, "Convective heat transfer and resistance characteristics of nanofluids with cylindrical particles," *Heat Transf. Eng.*, vol. 39, no. 6, pp. 526–535, 2018. DOI: 10.1080/01457632.2017.1320166.
25. M. Ghanbarpour, E. B. Haghigi, and R. Khodabandeh, "Thermal properties and rheological behavior of water based Al_2O_3 nanofluid as a heat transfer fluid," *Exp. Therm. Fluid sci.*, vol. 53, pp. 227–235, 2014. DOI: 0.1016/j.expthermflusci.2013.12.013. DOI: 10.1016/j.expthermflusci.2013.12.013.
26. M. Karimzadehkhouei *et al.*, "Experimental and numerical investigation of inlet temperature effect on convective heat transfer of γ-Al_2O_3/water nanofluid flows in microtubes," *Heat Transf. Eng.* vol. 40, pp. 738–752 [Published Online], Mar. 2018. DOI: 10.1080/01457632.2018.1442305.
27. G. S. Bhattacharjee, and W. L. Grosshandler, "The formation of wall jet near a high temperature wall under microgravity environment," *ASME, Heat Transf. Div.*, vol. 96, pp. 711–716, Jan. 1988.
28. S. Petrescu, "Comments on the optimal spacing of parallel plates cooled by forced convection," *Int. J. Heat Mass Transfer*, vol. 37, no. 8, pp. 1283, 1994. DOI: 10.1016/0017-9310(94)90213-5.
29. A. Bejan, and S. Lorente, *Design with Constructal Theory*. Hoboken, NJ, USA: J. Wiley and Sons, Inc., 2008.
30. B. C. Pak, and Y. I. Cho, "Hydrodynamic and heat transfer study of dispersed fluids with submicron metallic oxide," *Int. J. Exp. Heat Transfer*, vol. 11, no. 2, pp. 151–170, 1998. DOI: 10.1080/08916159808946559.
31. J. P. Meyer, S. A. Adio, M. Sharifpur, and P. N. Nwosu, "The Viscosity of Nanofluids: A Review of the Theoretical, Empirical, and Numerical Models," *Heat Transf. Eng.*, vol. 37, no. 5, pp. 387–421, 2016. DOI: 10.1080/01457632.2015.1057447.
32. F. P. Incropera, D. P. Dewitt, T. L. Bergman, and A. S. Lavine, "Thermophysical properties of Matter," in *Fundementals of Heat and Mass Transfer*, 6th ed. U.S. State, New York: J. Wiley, 2002, Appendix A, pp. 927–959.
33. S. K. Das, N. Putra, P. Thiesen, and W. Roetzel, "Temperature dependence of thermal conductivity enhancement for nanofluids," *J. Heat Transfer*, vol. 125, no. 4, pp. 567–574, 2003. DOI: 10.1115/1.1571080.
34. *COMSOL Multiphysics, Version 5.0*. Burlington, MA: COMSOL Inc, 2014.
35. T. Bello-Ochende, J. P. Meyer, and F. U. Ighalo, "Combined numerical optimization and constructal theory for the design of microchannel heat sinks," *Numer. Heat Transfer, Part A*, vol. 58, no. 11, pp. 882–899, 2010. DOI: 10.1080/10407782.2010.529036.
36. W. A. Khan, J. R. Culham, and M. M. Yovanovich, "Performance of shrouded pin-fin heat sinks for electronic cooling," *J. Thermophys. Heat Transfer*, vol. 20, no. 3, pp. 408–414, 2006. DOI: 10.2514/1.17713.